Atmospheric Environment 275 (2022) 119008

Contents lists available at ScienceDirect

Atmospheric Environment

journal homepage: www.elsevier.com/locate/atmosenv

Field calibration of a low-cost sensors network to assess traffic-related air pollution along the Brenner highway

Andrea Bisignano [a,*], Federico Carotenuto [b], Alessandro Zaldei [b], Lorenzo Giovannini [a]

[a] Department of Civil, Environmental and Mechanical Engineering (DICAM), University of Trento, Via Mesiano 77, 38123, Trento, Italy
[b] National Research Council. Institute for BioEconomy (CNR-IBE), Via Caproni 8, 50145, Firenze, Italy

HIGHLIGHTS

- Deployment and test of a low-cost sensors network for NO_2 alongside the Brenner highway.
- Development of a multivariate regression with two temperature-dependent classes of coefficients.
- Good agreement with reference instruments throughout a year-long validation.
- Data analysis shows the relation between valley winds and concentration patterns.
- Operational employment of low-cost sensors as a counter-check for the concentration values estimated by a dispersion model.

GRAPHICAL ABSTRACT

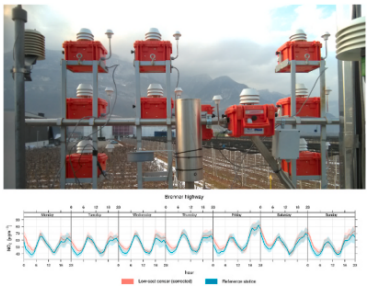

ARTICLE INFO

Keywords:
Traffic air pollution
Low cost sensors
Measurement uncertainty
Multivariate regression
NO_2 concentration
Valley wind system

ABSTRACT

This paper presents the results of a field campaign aiming at testing the ability of a network of low-cost electrochemical sensors to measure nitrogen dioxide concentration levels alongside one of the major Italian highway arteries. The results of a double on-field calibration, allowing for investigating the performance of the sensors under a broad range of weather conditions, are first shown and discussed. Different regression models are tested and their performance is widely assessed. Then, the measurements of the calibrated sensors are analyzed during a year-long field campaign, testing their performance against reference air quality stations and paying particular attention to different statistical indices. Results show a satisfactory performance of the low-cost sensors, highlighting their suitability to complement measurements from standard air quality stations, to reach a wider spatial coverage and to monitor pollutant concentrations in critical situations, when standard measurements are usually not feasible. Moreover, the dataset available from the year-long field campaign allows to extensively investigate nitrogen dioxide concentrations alongside the highway, pointing out in particular the strict relationship between pollutant concentration patterns and meteorological phenomena typical of Alpine valleys, such as daily-periodic thermally-driven wind systems.

* Corresponding author.
E-mail addresses: andrea.bisignano@unitn.it (A. Bisignano), federico.carotenuto@ibe.cnr.it (F. Carotenuto), alessandro.zaldei@ibe.cnr.it (A. Zaldei), lorenzo.giovannini@unitn.it (L. Giovannini).

https://doi.org/10.1016/j.atmosenv.2022.119008
Received 11 February 2021; Received in revised form 10 February 2022; Accepted 15 February 2022
Available online 23 February 2022

1. Introduction

Abbreviations

EU	European Union
MOSS	Metal oxide semiconductor sensor
ECS	Electrochemical sensor
APPA-TN	Environmental Protection Agency of Province of the Autonomous Trento
APPA-BZ	Environmental Protection Agency of Province of the Autonomous Bolzano
WMO	World Meteorological Organization
AQ	AirQino
MR	Multivariate regression
T-MR	Temperature-dependent multivariate regression
SP	Spline interpolation
RF	Random Forest
OOB	Out-of-bag
CORR	Correlation coefficient
NSME	Normalised mean square error
FB	Fractional bias
FAC2	Fraction within a factor of two
MB	Mean bias
MGE	Mean gross error
NMB	Normalised mean bias
NMGE	Normalised mean gross error
RMSE	Root mean squared error
COE	Coefficient of efficiency
IOA	Index of agreement
CQ	Conditional quantile

Over the last few years the increasing use of low-cost sensors for air pollution monitoring has generated a large debate, mainly concerning their actual reliability. The main weak spots of low-cost sensors (Karagulian et al., 2019; Concas et al., 2021; Clements et al., 2017; Spinelle et al., 2013; Popoola et al., 2016) are:

- lower accuracy than traditional reference instruments;
- need for frequent and location-specific calibrations;
- high sensitivity to atmospheric variables (especially humidity and temperature);
- cross-sensitivity to other gases;
- slow response with time-varying pollutant concentrations;
- drift and degradation.

Nevertheless, in environmental monitoring, a high-resolution sampling, both spatially and temporally, is essential to obtain representative information of air quality conditions and a complete understanding of the processes under study. Traditional approaches for monitoring air pollution generally make use of very expensive, complex, stationary equipment, which limits data collection (Watson et al., 1995). Hence, in order to monitor the pollution level in a given region, air quality stations are generally located at a few points where the highest concentration is expected, namely near the emission sites, like specific chimneys or major roads, along with some monitoring points accounting for background concentrations from minor and distributed pollution sources (EPA-AU, 2008). On the other hand, thanks to their reduced cost, size and consumption, new low-cost sensors allow the installation of denser monitoring networks for integrating the limited information on the spatial distribution of air pollutants provided by traditional measurements (Spinelle et al., 2015, 2017; Zikova et al., 2017a,b; Popoola et al., 2018; Borrego et al., 2016; Heimann et al., 2015).

In the present work, the potentiality of low-cost sensors to monitor air quality close to major roads and to evaluate the effects of mitigation strategies aiming at reducing vehicles' emissions is assessed. Actions aiming at reducing pollutant emissions from transport have increased over recent years in Europe, in order to improve air quality conditions. In particular, thanks to increasingly strict emission standards for vehicles, emissions from this sector have decreased since 1990, despite an increase of traffic fluxes. Between 1990 and 2017, emissions of NO_x from transport decreased by 40%, those of SO_x by 66%, and those of CO and non-methane VOCs by 87%. Between 2000 and 2017, emissions of PM2.5 decreased by 44% (EEA, b). Nevertheless, road transport is yet the major responsible for NO_x emissions, considering especially diesel cars. As a consequence, NO_2 concentrations often exceed the annual standard limit of 40 $\mu g\ m^{-3}$ close to major roads in many European countries (EEA, b). Hence, different policies are implemented in European states in order to reduce NO_x emissions and improve air quality, including reduced speed limits (EEA, a). Reduced speed limits are effective not only in reducing NO_x emissions, but also for non-exhaust releases from tires, brakes, and road abrasion, which contribute to emissions of primary PM2.5. However, in Italy this policy cannot be applied, as the enforcement of speed limits for environmental purposes is currently not allowed by the Italian road traffic code. In this context, the EU LIFE BrennerLEC project[1] aims at testing the effects of reduced speed limits on NO_2 concentrations. The final goal of the project is to implement a "low emission corridor (LEC)" for the A22 highway, which carries the heaviest traffic load in the whole Alpine region, with 11.1 million vehicles crossing the Brenner Pass between Austria and Italy in 2019. At a regional level, traffic on the A22 highway causes 41% of NO_x road transport emissions, which in turn is responsible for 60% of the total NO_x emissions. In the project, a proactive system for the management of speed limits based on current and predicted meteorological, air quality and traffic conditions has been developed. Moreover, in the framework of BrennerLEC, an extensive experimental campaign was carried out in order to assess the benefits associated to speed reduction. This includes traditional air quality monitoring stations, for both (urban and rural) background and for highway-related emissions, as well as a supplementary network of low-cost sensors, in order to improve the spatial coverage of air quality data. In the present work, an in-depth analysis of the performance of the low-cost sensors is presented, analyzing in particular data from two in-field calibrations (summer and winter periods) and from a year-long outdoor validation. It is worth highlighting that an outdoor evaluation of the performance of this kind of sensors over one year is a rare case in the literature. Here the focus is on NO_2, which is the most significant traffic-related air pollutant. The main aim is to investigate the long-term reliability of low-cost sensors in monitoring roadside NO_2 concentrations under different meteorological conditions and to highlight the potentiality of a dense network of sensors to capture peculiar roadside dispersion patterns. In the BrennerLEC project, the dynamic management of the speed limits is based on the air quality conditions predicted by means of a dispersion model; long-term performance assessment of low-cost sensors is crucial because they are employed operationally as a counter-check for the concentration values estimated by the model. The paper is organized as follows. Section 2 presents the field campaign and the study area, as well as the methodology adopted for the calibration of the low-cost sensors. The results of

[1] This research was funded by the LIFE program, grant number LIFE15 ENV/IT/000281, through the "BrennerLEC" project.

Table 1
Main characteristics of the low-cost sensors adopted to measure NO_2 concentrations in the BrennerLEC project.

Sensor	Range ($\mu g\ m^{-3}$)	Precision ($\mu g\ m^{-3}$)	Calibration (month)
MiCS-2710	94–9400	9	Every 12
NO2-A43F	0–1880	9	Every 12
Sens-IT	20–470	19	Every 6

the calibration are presented in Section 3, while Section 4 shows the performance of the sensors during the year-long field campaign. In Section 5 data from the low-cost sensors are analyzed in order to characterize NO_2 concentrations along the A22 highway. Finally, conclusions are presented in Section 6.

2. Materials and methods

2.1. Choice of the low-cost sensor technology

Detectors for monitoring nitrogen dioxide can be based on different technologies: currently available sensors include metal oxide semiconductor, electrochemical, infrared and photo-ionisation detector sensors. Both metal oxide semiconductor and electrochemical detectors are employed in the BrennerLEC project, as they are the least expensive and most widely used technologies in low-cost sensing units. Metal oxide semiconductor and electrochemical sensors (hereinafter MOSSs and ECSs respectively) present similar characteristics considering both price, being inexpensive compared to traditional chemiluminescence sensors used in official air quality stations, and the relatively high sensitivity, which allows measurements in ambient air. Moreover, both types of sensors have small size, which allows the possibility to install them also close to major roads. ECSs require lower power draw than MOSSs, as the latter need an electric heater. On the other hand, MOSSs have generally a longer lifespan and higher resilience against weather conditions than ECSs. In general, sensitivity is affected by atmospheric conditions and by other gases for both of them, even if the sensitivity of ECSs is less influenced by temperature and humidity than for MOSSs (Concas et al., 2021). However, low humidity and high temperatures can dry out the electrolyte and damage the detector.

For the BrennerLEC field campaign we adopted the MOSSs Sens-IT (Unitec, 2018) and MiCS-2710 (e2v, 2008) sensors, and the ECSs Alphasense NO2-A43F sensor (Alphasense, 2019). Table 1 shows the main characteristics of the three sensors, referring to nitrogen dioxide measurements; range and precision specifications are obtained from the manufacturer's data-sheets (Unitec, 2018; e2v, 2008; Alphasense, 2019), while the calibration interval from the literature review provided by Concas et al. (2021).

A preliminary analysis of the data collected from these sensors highlighted that the Alphasense NO2-A43F presents the best performance in measuring NO_2 concentrations when compared with reference measurements. Therefore, the results presented in this work, including the calibration and the year-long measurements campaign, focus on the measurements performed with this kind of sensors only.

2.2. AirQino sensors board

AirQino (hereinafter AQ) is a custom-made printed circuit board (PCB) developed by the Institute of BioEconomy of the Italian National Research Council (CNR-IBE). The board integrates a set of commercial low-cost sensors for various meteorological, aerosol and gaseous measurements and acts as an Arduino shield allowing for flexible sampling programming. The PCB integrates sensors for air temperature and relative humidity (AM2315 Adafruit, New York City, NY, USA), particulate matter concentration (SDS011, Nova Fitness, Jinan, China) and CO_2 (S8, SenseAir, Delsbo, Sweden). The board also integrates a set of sensors for gaseous pollutants such as CO (TGS-2600, Figaro Inc., Arlington Heights, IL, USA), total VOCs (MiCS-5524, SGX Sensortech, Neuchatel, Switzerland), NO_2 (MiCS-2710, SGX Sensortech) and O_3 (MiCS-2614, SGX Sensortech). For the BrennerLEC application, auxiliary NO (NO-A4, Alphasense, Great Notley, Essex, United Kingdom) and NO_2 (NO2-A43F, Alphasense) sensors were added to the AirQino board. AQ is also equipped with a GPS unit and a General Packet Radio Service (GPRS) modem, allowing for precise time-stamping, geo-localization of the measurements and data transmission to a centralized server. Finally, a watchdog module is used to reset the processing unit of the AQ every 24 h to bypass eventual software failures. The whole electronics and sensors are enclosed in a waterproof box where air circulation is guaranteed by two Ingress protection (IP) 33 ventilation devices (mod. 3540631, Fibox Inc., Glen Burnie, MD, USA) and a MC20080V1 brushless fan (Sunon Inc., Brea, CA, USA) with a nominal flow-rate of 2.7 $m^{-3}\ h^{-1}$. To accurately measure air temperature and relative humidity the relevant sensor is exposed through the box, but thoroughly protected with a radiation shield. Similarly, the particulate matter sensor has a separate inlet and an internal fan able to provide continuous air circulation at 0.75 $m^3\ h^{-1}$. The system is directly powered by 220 V AC power through a 12 V AC-DC transformer and it then redistributes a steady 5 V DC power to the electronics through an internal DC-DC converter. Power consumption is 200 mA - 12 V DC, about 2.5 W. AQ performance was tested against reference sensors in both urban and extreme environments with satisfying accuracy (Zaldei et al., 2017; Gualtieri et al., 2017; Cavaliere et al., 2018; Carotenuto et al., 2020).

2.3. Reference air quality stations

Three reference monitoring stations were installed alongside the A22 highway at a distance of 8 m from the traffic lane centerline. They are equipped with meteorological sensors and reference gas analysers for NO, NO_2, NO_x O_3, CO and particulate matter. Measurements are carried out in parallel to the low-cost sensors, as discussed in the next sections. Two stations (ML103 and ML107) are managed by the Environmental and Climate Protection Agency of the Autonomous Province of Bolzano (APPA-BZ) and one (BL164) by the Environmental Protection Agency of the Autonomous Province of Trento (APPA-TN). Both agencies are partner of the BrennerLEC project. The reference measurements of NO_2 are used for the calibration of the low-cost sensors, data validation and comparison. All three stations monitor atmospheric NO, NO_2 and NO_x concentrations using the Horiba APNA-370 detector (Horiba). APNA-370 is included in the "List of Designated Reference and Equivalent Methods" of the United States Environmental Protection Agency for measuring ambient concentrations of NO_2 (EPA-US, 2020). The working principle is a cross-flow modulated semi decompression chemiluminescence method. It employs an internal dry-method sampling device to achieve the highest levels of sensitivity and accuracy. The stations measure also the principal meteorological parameters, including air temperature and relative humidity, atmospheric pressure, rainfall, wind speed and direction, and solar radiation. APPA-TN employs a Davis Vantage Pro2 weather station, while APPA-BZ uses SIAP + MICROS sensors. Both are compliant with the standards of the World Meteorological Organization (WMO, 2018).

2.4. Set-up of the field campaign and data collection

The A22 (or Brenner) highway, which connects the Po Plain to Austria through the Brenner Pass, is one of the most important Italian and European motorways, representing in particular the busiest Alpine corridor. It is a crucial connection for transports between southern and northern Europe by moving approximately 40′000 vehicles per day, with higher peaks during holidays. Considering the economical impact of this infrastructure, it is estimated that more than 30 million tonnes of freight are transported by road along the Brenner corridor each year (Cavallaro and Sommacal, 2018).

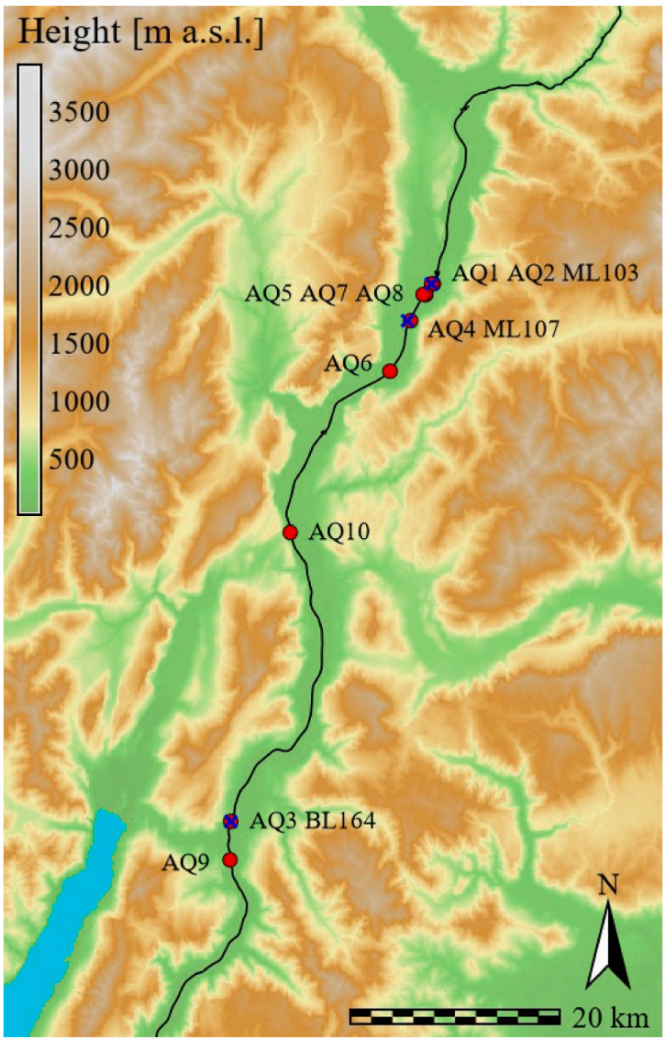

Fig. 1. Map of the study area showing the A22 highway (black line), the position of the AQ sensors (red circles) and of the official air quality stations (blue crosses). (For interpretation of the references to color in this figure legend, the reader is referred to the Web version of this article.)

Table 2
Main information on the positioning of the low-cost sensors and of the reference air quality stations.

Tag	Location (km)	Carriageway	Elevation (m)
AQ1	103.7	South	4
AQ2	103.7	North	4
AQ3	164.4	South	4
AQ4	107.8	North	4
AQ5	105.2	North	10
AQ6	132.8	South	4
AQ7	105.2	South	10
AQ8	105.2	North	4
AQ9	167.9	South	4
AQ10	113.4	North	4
ML103	103.7	South	3.1
ML107	107.8	South	3.4
BL164	164.4	South	3.95

A22 is a dual carriageway consisting of two lanes of traffic in each direction (with the lane nearest to the center being reserved for overtaking) and two hard shoulders on the sides. Each lane is about 4 m wide and the shoulders around 3 m. The Brenner highway is 315 km long, but in the present work we consider a stretch of about 60 km (from Egna-Ora to Rovereto South), where 10 AQ sensors were installed. Here the A22 highway follows the floor of the Adige Valley, which is north/south oriented and has a fairly constant width of 2–3 km, with adjacent mountain peaks reaching heights around 2000 m above the valley floor (Fig. 1). The AQ sensors were installed in fixed positions alongside the highway at heights between 4 and 8 m above ground level and at a horizontal distance of 8 m from the traffic lane centerline. The field campaign started in 2018 and in the present work data from a full year, from March 2019 to February 2020, are considered.

The 10 low-cost sensors allowed us to collect a comprehensive spatio-temporal dataset, which was complemented by traffic data coming from several inductive loops measuring vehicles number and velocity. Table 2 summarizes the main information on the location of the AQ sensors and of the reference air quality stations.

Note that the position of the sensors is marked by the distance from the Brenner Pass expressed in kilometers, as usual for highways. Also the air quality stations acronyms (ML103, ML107 and BL164) contain the distance from the Brenner Pass. All the sites were selected to guarantee that observations are as much as possible representative of a large area and not significantly affected by local effects. In particular, the location of the AQ sensors has been selected in homogeneous and straight stretches of the highway, with no tollbooths and service stations nearby, as they may significantly influence cars velocity and, consequently, emissions rates. Moreover, sensors were installed far from industrial or residential areas, which may affect local pollutant concentrations introducing additional emissions. Two AQ sensors (AQ1 and AQ3, at km 103.7 and 164.4 respectively) were installed on the roof of two reference air quality stations, ML103 and BL164, along the south carriageway (southward flow of traffic), allowing for a direct comparison of NO_2 measurements. On the other hand, the comparison of the measurements of the low-cost sensor installed at km 107.8 on the North carriageway (AQ4) with the reference observations performed at ML107 on the other side of the highway allows to evaluate the effects of local meteorological conditions on pollutant dispersion on both sides of the road. A similar comparison can be performed also at km 103.7. At km 105.2, the presence of two AQ sensors at different heights (4 m and 10 m) permits to investigate also the variation of pollutant concentrations with elevation.

AQ sensors collect data with a 2-min time resolution and, through General Packet Radio Service (GPRS) technology, they send geolocated measures to a web application server allowing to visualize, manipulate and share real-time information. Raw data collected by the AQ sensors are aggregated into hourly averages so as to make data analysis more robust.

Air quality and meteorological measurements at the reference stations are registered at 10-min intervals. Also in this case hourly averages are calculated for a direct comparison with the AQ sensors.

2.5. *Meteorological characteristics of the site*

The highway lies on the floor of the Adige Valley, where the patterns of pollutant concentrations are expected to be strictly related to atmospheric processes typical of Alpine valleys (Tomasi et al., 2019; Falocchi et al., 2020; Giovannini et al., 2020). In particular, the main factors affecting pollutant dispersion in the Adige Valley are the development of strong and frequent thermal inversions at night, especially during wintertime (Tomasi et al., 2017), and the presence of a valley wind system, especially in spring and summer (Giovannini et al., 2017). As a consequence, higher pollutant concentrations are expected in the cold months, due to the reduced mixing induced by the stable stratification characterizing the valley atmosphere in this period. On the other hand, valley winds, which typically blow down-valley (northerly winds) at night and in the first part of the morning and up-valley (southerly winds) from late morning to early evening, are expected to strongly influence the diurnal cycle of pollutant concentrations. The presence of a well-developed valley wind system in the Adige Valley can be clearly appreciated from the wind roses at the three reference air quality

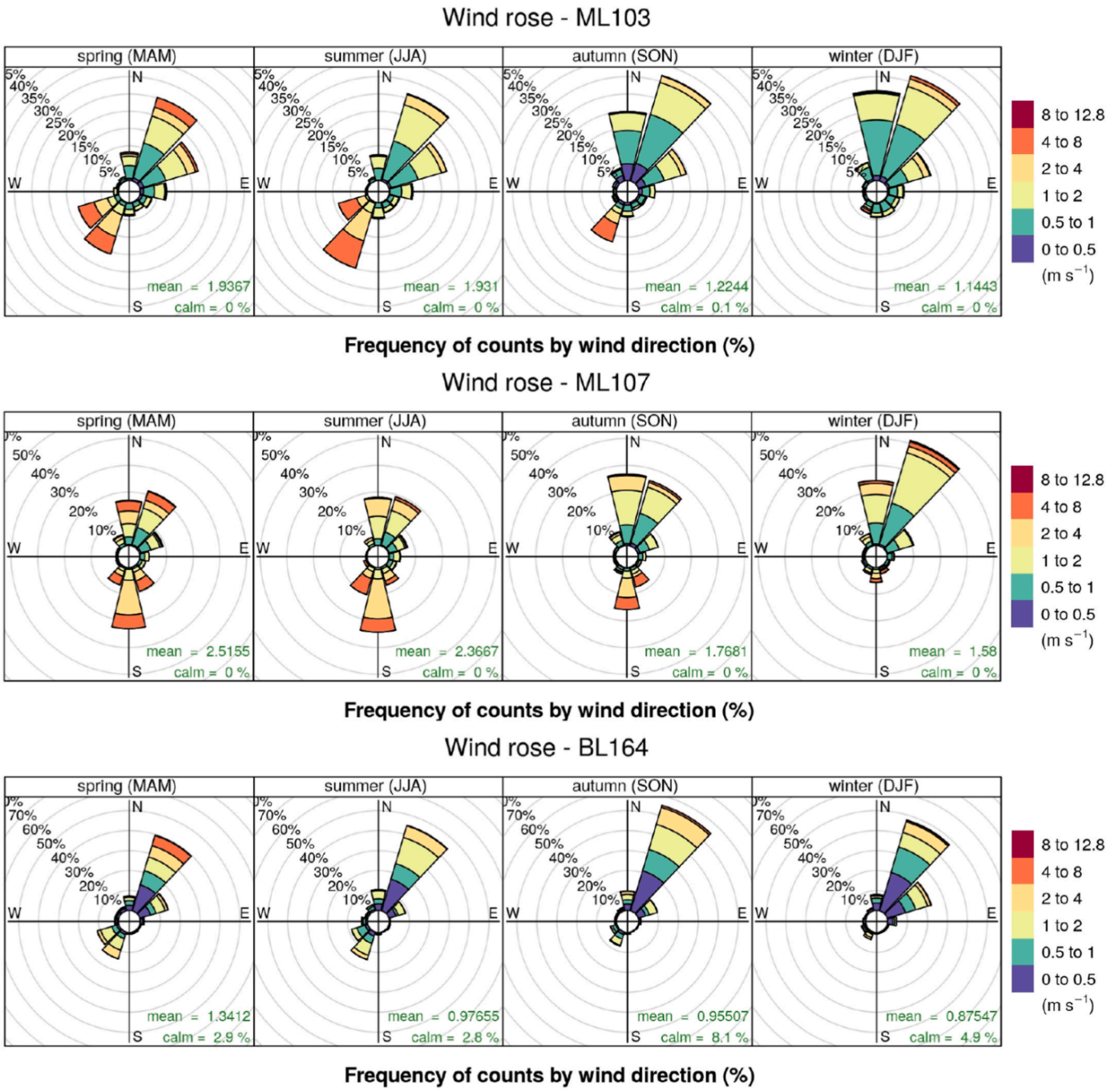

Fig. 2. Wind roses at ML103, ML107 and BL164 reference stations.

stations reported in Fig. 2. Wind direction is always aligned with the valley axis, marking the direction of down- and up-valley winds. In spring and summer both down- and up-valley winds are well developed, while in winter northerly (downvalley) winds are predominant, since in this season the solar radiation is too weak for the development of the thermal contrasts driving up-valley winds (Giovannini et al., 2017).

2.6. Calibration models

Two field campaigns were carried out in order to calibrate the AQ sensors. The first field calibration was carried out in June 2018 on the rooftop of an operational APPA-TN air quality station, in the city of Trento, close to a major suburban road. The 10 AQ sensors were installed side by side and data were collected during the whole month of June 2018. A second period of calibration was required to test the sensors under a wider range of climatic conditions. It took place in the first two weeks of February 2019 and the AQ sensors were installed on the roof of the reference station ML103. The winter field calibration allowed to calibrate the AQ sensors under higher NO_2 concentrations and different weather conditions, such as lower temperatures and higher relative humidity. The hot- and cold-season calibration data (a total of 6 weeks) were merged and jointly used to find the best regression curve.

We tested four calibration models, i.e. two multivariate regressions, a spline interpolation and a random forest algorithm, using the R open-source software, version 3.6.3 "Holding the Windsock" (R-Team, 2006), for implementation and validation.

The first method is a simple multiple linear regression, the extension of a classical linear least-squares regression involving n explanatory

variables:

$$y_{ij} = \sum_{k=0}^{n} x_{ik}\alpha_{kj} + \varepsilon_{ij} \quad (1)$$

where y_{ij} is the i-th NO_2 reference measurement ($NO2_{-ref}$) for the j-th sensor, x_{ik} is the i-th value of the k-th explanatory variable, α_{kj} is the regression coefficient of the k-th explanatory variable for the j-th sensor and ε_{ij} is the residual. Note that $x_{i0} = 1$ implies α_{0j} to be the regression intercept.

Several works adopting multivariate regressions for the calibration of low-cost sensors highlighted that the addition of temperature (T) and relative humidity (RH) to the explanatory variables of the model generally improves significantly the accuracy of the calibration (Spinelle et al., 2015; Masson et al., 2015; Piedrahita et al., 2014; Popoola et al., 2016; Borrego et al., 2016). Mijling et al. (2018) showed that the models including T as explanatory variable outperform the ones including RH. Moreover, the same study highlighted that, when both variables are used as predictors, the accuracy of the calibration was very similar to the one obtained adopting only T. Preliminarily calibration tests performed in the present work confirmed these findings, highlighting that the sensor response depends more strongly on T than on RH, and that the two variables are colinear (Alphasense, 2019; Mijling et al., 2018). In particular, the inclusion of RH among the explanatory variables did not improve the results significantly. Hence, RH was not considered for the calibration in the present work. Most literature studies adopt ambient air temperature as explanatory variable (Popoola et al., 2016). Here we decided to adopt the internal air temperature measured by the AQ sensors (T_{int}), as this is the temperature directly affecting the sensor behavior. We observed that the internal sensor temperature is about 4 °C higher than the ambient temperature all the year through, while being roughly equivalent in trends. Hence their effect as explanatory variable in the regression is highly comparable as well.

We investigated the influence of all the available variables on NO_2 measurements and found that only the inclusion of ozone (O_3) as explanatory variable improved significantly the results. O_3 is directly measured by the AQ platform. Considering raw NO_2 data ($NO2_{-raw}$), we found that the best results were obtained using a second degree polynomial of $NO2_{-raw}$. Hence, we modeled the final calibration curve as a multivariate regression (MR), including a (quadratic) polynomial regression and a multiple linear regression:

$$NO_{2-ref} = \alpha_0 + \alpha_1 NO^2_{2-raw} + \alpha_2 NO_{2-raw} + \alpha_3 O_3^{0.1} + \alpha_4 T^4_{int} \quad (2)$$

where the indexes i and j are omitted for sake of simplicity. The exponents in the explanatory variables of the linear part of Eq. (2), namely $O_3^{0.1}$ and T^4_{int}, were calculated from two separate, prior power regression models. We applied the ordinary method of (non-linear) least squares to calculate the calibration coefficients. The constant terms of the quadratic and multiple linear regressions merge into the α_0 addend. It is worth noting that only variables measured by the AQ platform have been used for the calibration, thus allowing the results obtained in the present work to be extended also to other contexts, being independent from external measurements.

The second method uses the same MR shown in Eq. (2). The difference lies in the calculation of the α coefficients. We noticed that α values vary significantly if the two calibration periods are considered separately. Hence, we calculated two different sets of the α coefficients for the summer and the winter periods. The criterion for choosing the set of α coefficients is simply based on the internal temperature (T_{int}) measured by the AQ sensors. In particular, we found that the best cutoff value is $T_{int} = 20°C$. Therefore, in this second approach (T-MR), we apply two multivariate regressions, depending on the value of the internal temperature measured by the AQ sensors.

Although MR and T-MR allow for a quadratic regression between $NO2_{-raw}$ and $NO2_{-ref}$, the two models are still considered a linear regression since they are linear in the regression coefficients. It is worth noting that a MLR may include any interaction term between the predictors, even without one of them being a polynomial of the others.

Table 3
Statistical performance indexes for the calibration models.

CORR				
Tag	MR	T-MR	SPL	RF
AQ1	0.77	0.93	0.93	0.92
AQ2	0.84	0.89	0.95	0.93
AQ3	0.94	0.97	0.97	0.96
AQ4	0.95	0.96	0.97	0.96
AQ5	0.93	0.95	0.96	0.95
AQ6	0.61	0.89	0.94	0.94
AQ7	0.89	0.94	0.95	0.94
AQ8	0.87	0.89	0.94	0.93
AQ9	0.90	0.96	0.97	0.96
AQ10	0.89	0.92	0.94	0.93
NMSE				
Tag	MR	T-MR	SPL	RF
AQ1	0.14	0.05	0.05	0.06
AQ2	0.10	0.07	0.04	0.05
AQ3	0.04	0.02	0.02	0.03
AQ4	0.04	0.03	0.02	0.03
AQ5	0.04	0.03	0.03	0.03
AQ6	0.21	0.07	0.04	0.04
AQ7	0.07	0.04	0.04	0.04
AQ8	0.08	0.07	0.04	0.05
AQ9	0.07	0.03	0.02	0.03
AQ10	0.07	0.05	0.04	0.04
FAC2				
Tag	MR	T-MR	SPL	RF
AQ1	0.89	0.93	0.94	0.93
AQ2	0.93	0.96	0.97	0.97
AQ3	0.97	0.98	0.99	0.98
AQ4	0.97	0.98	0.98	0.97
AQ5	0.97	0.97	0.98	0.98
AQ6	0.81	0.95	0.98	0.97
AQ7	0.93	0.97	0.98	0.97
AQ8	0.94	0.96	0.97	0.97
AQ9	0.95	0.98	0.98	0.98
AQ10	0.94	0.96	0.97	0.97

The third method is based on a spline interpolation (SP) (Fritsch and Carlson, 1980; Chambers et al., 1990). In particular, we generated a cubic B-spline regression using the same predictor variables as in the MR. The method generates a basis matrix for representing the family of piecewise polynomials with the specified internal breakpoints and degree, evaluated at the values of the predictor variable. This representation has the advantage that the estimation of the unknown function reduces to the estimation of the coefficients associated with the basis functions (Perperoglou et al., 2019).

Finally, the fourth method implements the Breiman's random forest (RF) algorithm (Breiman, 2001). Several works showed that a successful calibration of low-cost sensors can be achieved using machine-learning-based models, such as artificial neural networks and random forests (Spinelle et al., 2015; Zimmerman et al., 2018; De Vito et al., 2009; Esposito et al., 2016). Here the randomForest R package (Liaw and Wiener, 2014) was used in order to implement a multiple regression forest. Again, in order to allow a uniform comparison, $NO2_{-raw}$, O_3 and T_{int} were selected as predictors. In Breiman's algorithm a cross-validation or a test subset are not necessary to determine an unbiased estimate of the error, thanks to the out-of-bag (OOB) approach (Breiman, 2001; Boehmke and Greenwell, 2019). In OOB error estimate, each tree is built from a different bootstrap sample, i.e. a subset randomly selected with replacement from the original data. Each tree is trained on 63.2% of the data and the leftover 36.8% is used to assess the performance, similarly to cross-validation.

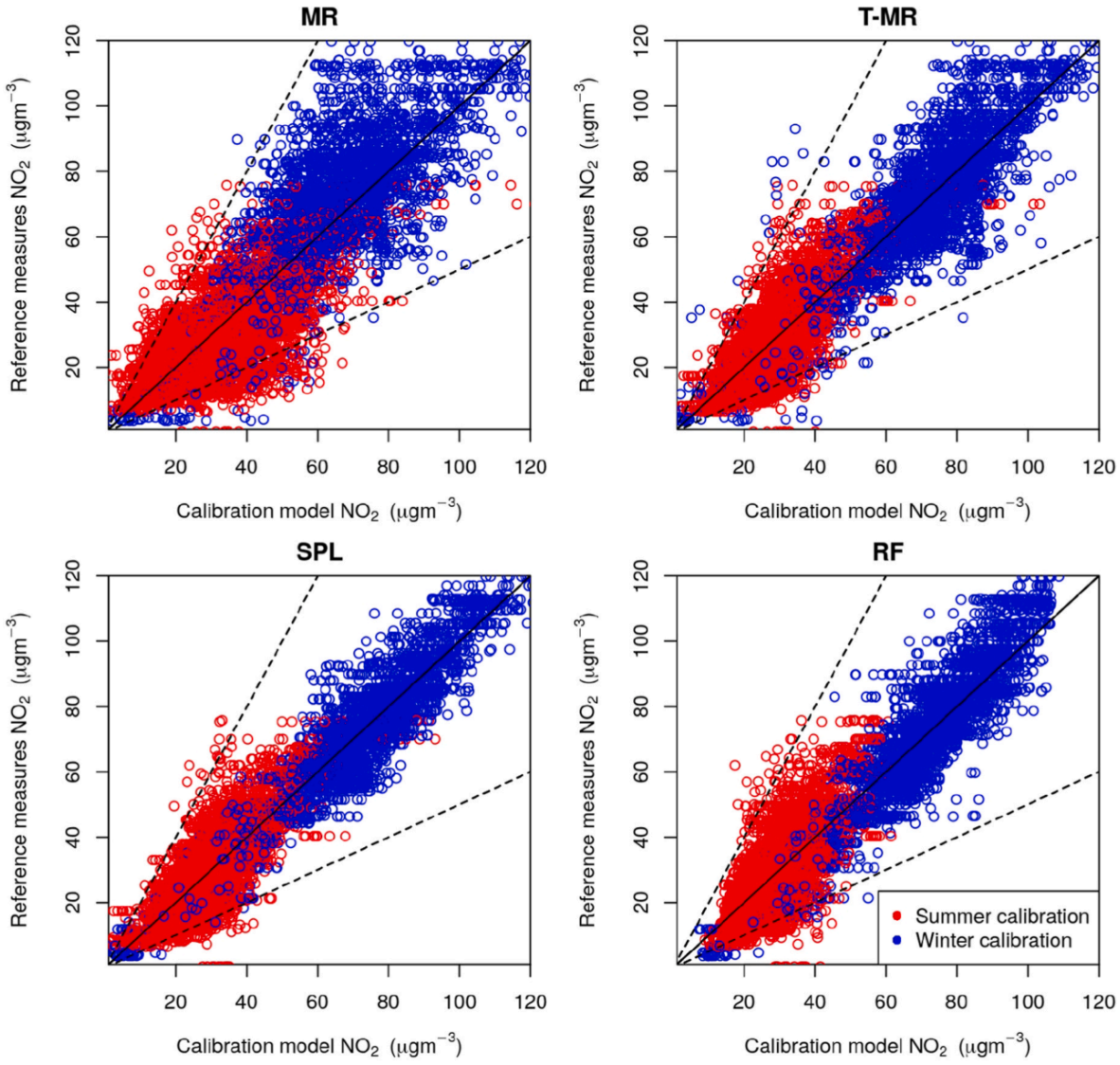

Fig. 3. Scatterplots of reference versus AQ calibrated NO_2 concentrations for the four models.

3. Performance of the calibration models

Several statistical indexes can be used to assess the accuracy of the predictions of a model (see for instance Patryl and Galeriu (2011); Thunis et al. (2012); Pederzoli et al. (2012); Chang and Hanna (2004, 2005) and, paying special attention to regressions, Spuler et al. (2015); Botchkarev (2019)). The calculation of multiple performance metrics is always recommended, as each index takes into account a particular aspect of the comparison between model predictions and observations. The performance metrics used here include the correlation coefficient (CORR), the normalised mean square error (NMSE) and the fraction of predictions within a factor of two of observations (FAC2). Other performance measures, i.e. the fractional bias (FB), the mean bias (MB), the mean gross error (MGE), the normalised mean bias (NMB), the normalised mean gross error (NMGE), the root mean squared error (RMSE), the coefficient of efficiency (COE) based on LeGates and McCabe (2013) and the index of agreement (IOA) based on Willmott et al. (2012), are presented in the supplementary material.

The data analysis presented hereinafter was carried out by means of the Openair R package (Carslaw and Ropkins, 2012; Carslaw, 2019), specifically developed for air pollution measurements. This package allows for data importation and manipulation, calculation of a wide range of statistical performance indexes and plot of different types of graphics (such as the Taylor diagram, the conditional quantile plot, the pollution rose and the polar plot), which can be useful for the interpretation of data. The values of CORR, NMSE and FAC2 are listed in Table 3, while the other performance metrics are reported in Table S1 of the Supplementary material.

SPL and RF models show very high correlation factors (always greater than 0.9) for all AQ sensors during the calibration period. T-MR improves significantly the correlation level obtained with MR, with values above 0.9, confirming the effectiveness of a temperature-dependent approach. The same is true for NMSE. Table 3 shows that T-MR indeed generates NMSE values smaller than MR, although not always reaching the low values of SPL and RF. FB is close to zero for all the calibration models and AQ sensors (Table S1, supplementary material), thus indicating the absence of systematic errors. However, good values for FB, CORR and NMSE are not sufficient conditions for a good model (Patryl and Galeriu, 2011). In fact, NMSE and FB are influenced by the possible occurrence of high observed and predicted values and CORR by the possible good match for a few extreme pairs (Chang and Hanna, 2005). On the other hand, the presence of outliers does not affect FAC2 values. FAC2 presents very similar values for T-MR, SPL and RF, while, also in this case, MR shows the worst performance, corroborating

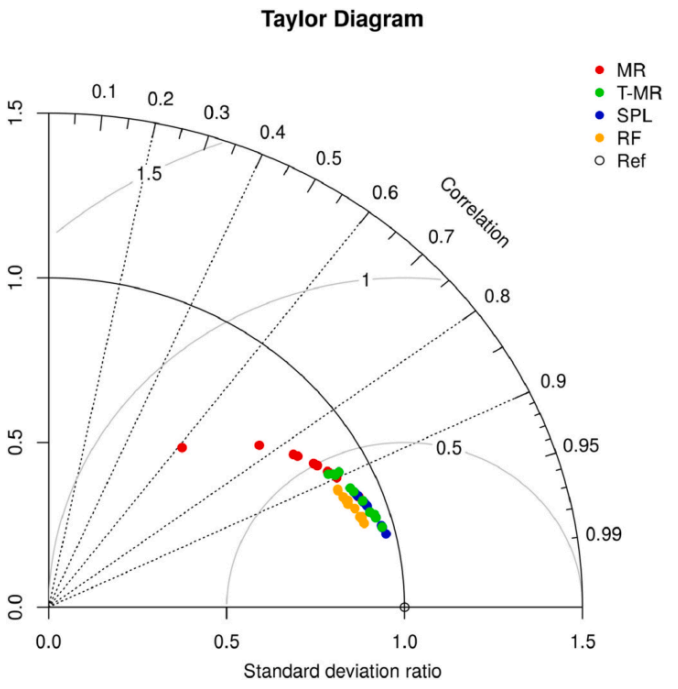

Fig. 4. Taylor diagrams of the calibration models predictions against the reference values.

the superiority of T-MR with respect to MR. The other performance metrics (Table S1, supplementary material) confirm once again that T-MR, SPL and RF models are effective in predicting the observations. For example, COE>0.6 implies that the absolute values of the differences between the observations and the model predictions are less than 40% of the difference between the observations and their mean and IOA>0.7 indicates that the sum of the error magnitudes is less than 30% of the sum of the observed deviation magnitudes (LeGates and McCabe, 2013; Willmott et al., 2012; Carslaw, 2019).

In order to further analyze the models performance, Fig. 3 shows the scatterplots of the reference measurements against the calibrated hourly concentrations for the four models. The red and blue dots indicate the summer and winter calibrations, respectively. The overall performance is satisfactory for all the four models, as almost all the points (>90%) are within the FAC2 curves (dashed lines), albeit the correlation decreases at the lowest values. Again, T-MR appears to be more accurate than MR, and comparable to SPL and RF.

The goodness of the calibration models has been evaluated also with the Taylor diagram (Taylor, 2001; Cordero et al., 2018; Carslaw, 2019) in Fig. 4.

Taylor diagram displays CORR (proportional to the polar angle from the *y* axis), the centered RMSE (proportional to the distance from the reference point, i.e. the grey arcs) and the standard deviation (the radial distance). It is worth pointing out that in Fig. 4 data are normalised, so as the standard deviation of NO_{2-ref} is 1. CORR and centered RMSE for T-MR, SPL and RF are very similar, while the standard deviation is slightly underestimated by RF. On the other hand, MR performs markedly worse than the other models for 6 of the 10 AQ sensors. On the basis of the statistical analysis of the performance of the different calibration models, it can be concluded that T-MR, SPL and RF present similar accuracy in reproducing the observed reference NO_2 values. However, given the simplicity of T-MR with respect to the other two methods, the former model is selected for the following environmental analyses. In fact, the aim of the BrennerLEC project is to adopt operationally the low-cost sensors to support the implementation of environmental policies, keeping the calibration technique as simple as possible. Hence, the T-MR method is adopted in the following analyses for the evaluation of the suitability of the low-cost sensors for monitoring NO_2 concentrations during the full year from March 2019 to February 2020.

Table 4
Statistical performance indexes for AQ1 and AQ3 for the year-long validation.

Sensor AQ1 vs Station ML103			
Time period	CORR	NMSE	FAC2
Entire year	**0.78**	**0.07**	**0.95**
March 2019	0.85	0.09	0.93
April 2019	0.68	0.16	0.93
May 2019	0.52	0.26	0.82
June 2019	0.71	0.15	0.92
July 2019	0.75	0.13	0.96
August 2019	0.67	0.13	0.95
September 2019	0.63	0.11	0.97
October 2019	0.52	0.16	0.95
November 2019	0.83	0.12	0.99
December 2019	0.91	0.04	0.99
January 2020	0.90	0.03	0.99
February 2020	0.84	0.05	0.98
Sensor AQ3 vs Station BL164			
Time period	CORR	NMSE	FAC2
Entire year	**0.79**	**0.08**	**0.93**
March 2019	0.90	0.10	0.93
April 2019	0.63	0.21	0.90
May 2019	0.64	0.19	0.90
June 2019	0.57	0.21	0.90
July 2019	0.57	0.23	0.85
August 2019	0.61	0.17	0.91
September 2019	0.58	0.17	0.93
October 2019	0.57	0.17	0.95
November 2019	0.78	0.22	0.91
December 2019	0.94	0.04	0.99
January 2020	0.93	0.04	0.99
February 2020	0.89	0.07	0.96

4. Long term validation

As mentioned above (Section 2.6), only AQ1 and AQ3 sensors were installed at the same location of the reference stations (ML103 and BL164 respectively), hence allowing for a direct comparison. Here we present the statistical evaluation of the performance of these two sensors, extended to the whole year of validation. Table 4 shows that the low-cost sensors measurements, adopting the T-MR model, compare reasonably well with the reference ones. As expected, the statistical indexes present slightly worse values with respect to the calibration periods, due to the fact that during the whole year the AQ sensors experienced levels of concentration and meteorological conditions far more variable with respect to the six-week calibration period. Possible small drifts of the NO_2, O_3 or T_{int} sensors may also explain the slight deterioration of the sensors performance. CORR and NMSE values slightly deteriorate with respect to the calibration, but still highlighting a good level of accuracy. On the other hand, FAC2 assumes fairly the same values as in the calibration period. Month-by-month values of the statistical indexes do not reveal a significant loss of accuracy throughout the year of validation; they rather show that the sensors consistently performed better in winter than summer (which will be discussed below). The same statistical performance indexes as in Table S1 are shown in Table S2 (supplementary material) for the year of validation, pointing out that the overall accuracy is still satisfactory for both sensors.

An overall satisfying behavior of AQ1 and AQ3 throughout the validation period can also be seen in the scatterplots presented in Fig. 5. AQ1 and AQ3 do not exhibit systematic errors, thus pointing out their long-term reliability. A long lifespan under a wide range of operating conditions is essential for making the low-cost sensors effective in monitoring air pollutants levels.

Finally, the performance of the low-cost sensors is also analyzed using conditional quantile (CQ) plots (Wilks, 2019; Carslaw, 2019) on a

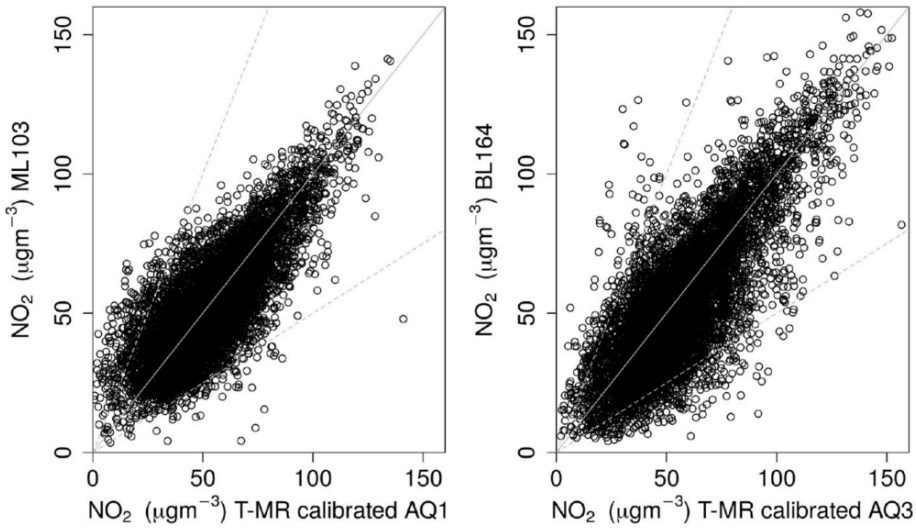

Fig. 5. Scatterplots of ML103 versus AQ1 (left panel) and BL103 versus AQ3 (right panel) NO_2 measurements throughout the year-long validation.

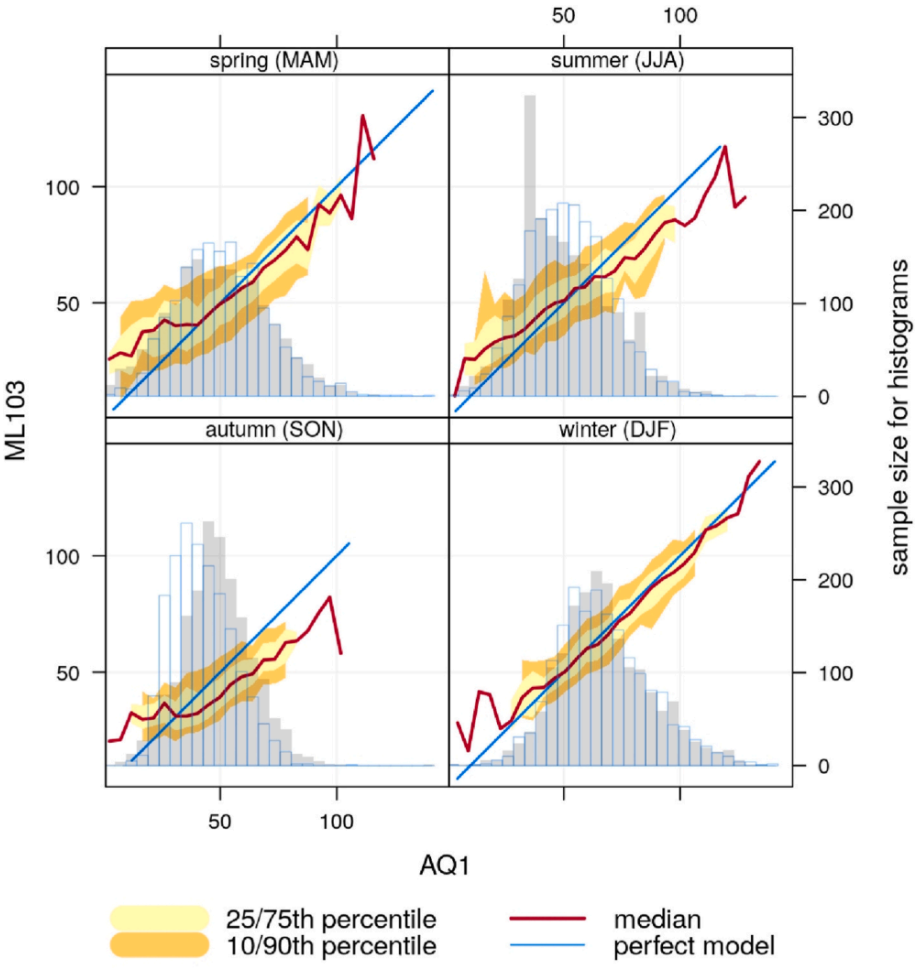

Fig. 6. Conditional quantile plot of ML103 versus AQ1 NO_2 measurements divided by season throughout the year-long validation.

seasonal basis (Figs. 6 and 7). In these diagrams, the reference measurements are split into bins according to the calibrated values of the low-cost sensors. The median of AQ values (red line), the 25/75th (yellow shading) and 10/90th (orange shading) quantile intervals are plotted in comparison to the diagonal (blue line), which represents a perfect model. The histograms in the lower part of the panels represent the counts of calibrated AQ (shaded grey) and reference (thin blue line) values. Considering AQ1, the best performance is reached in winter, when the median well matches the perfect model line, the spread in the quantiles is narrower and the two distributions are very similar. On the other hand, in spring, summer and autumn AQ1 tends to underestimate high concentrations and to overestimate low concentrations. Errors are

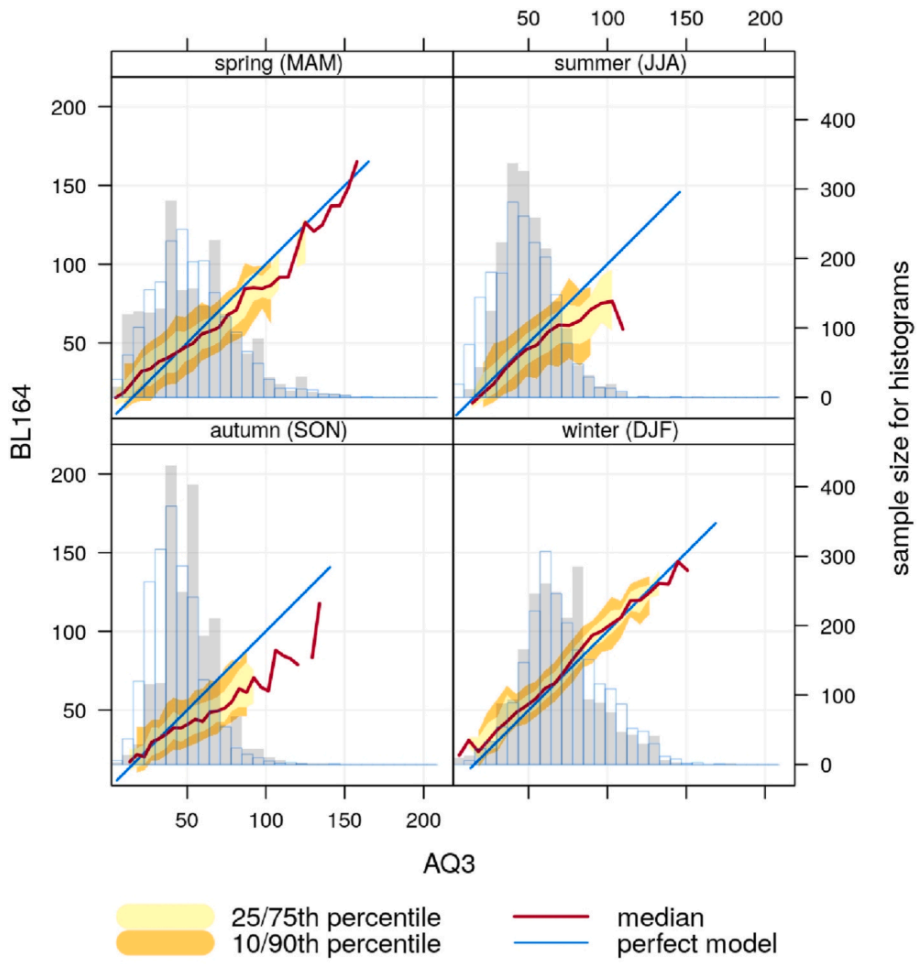

Fig. 7. Conditional quantile plot of BL164 versus AQ3 NO_2 measurements divided by season throughout the year-long validation.

Table 5
NO_2 mean values ($\mu g\ m^{-3}$) in the period March 2019–February 2020 measured by the AQ sensors and the reference air quality stations.

Sensor/Station	NO_2 concentration ($\mu g\ m^{-3}$)
AQ1	48–0
AQ2	49.5
AQ3	56.2
AQ4	48.9
AQ5	45.4
AQ6	48.8
AQ7	49.6
AQ8	44.8
AQ9	52.1
AQ10	52.4
ML103	51.6
ML107	48.8
BL164	53.3

more evident in autumn, when also the histograms of AQ1 and of the reference observations differ more significantly. The behavior is similar also for AQ3, but with a generally better agreement with the reference measurements in all the seasons. Fig. 7 also shows that in summer the median line overlaps the perfect model line for concentrations lower than 50 $\mu g\ m^{-3}$, while it tends to be below the diagonal for higher concentrations. The reason why the winter period shows the best agreement probably lies in the dual form of T-MR. During spring and autumn the internal temperature of the AQ sensors may oscillate around the cut-off value of 20 °C, enhancing the uncertainty. On the other hand, in winter and in summer T_{int} is always lower and higher than 20 °C, respectively. The difference between winter and summer performance is likely due to the fact that the winter calibration took place close to the highway and hence under working conditions more similar to those of the validation period. Furthermore, Alphasense NO2-A43F technical specifications (Alphasense (2019)) recommend a working temperature range of −30–50 °C. The sensors registered higher internal temperatures almost every day during summer, while not reaching the lower limit during winter.

5. Nitrogen dioxide concentrations close to the highway

In accordance with the EU air quality directive (2008/EC/50), the Italian decree-law 155/2010 provides two limit values for the protection of human health from exposure to NO_2. First, hourly concentrations cannot exceed 200 $\mu g\ m^{-3}$ more than 18 times in a year and, second, the annual mean value cannot exceed 40 $\mu g\ m^{-3}$. While the first law-limit is always respected also close to the motorway, Table 5 shows that yearly average concentrations (March 2019–February 2020) exceed 40 $\mu g\ m^{-3}$ for all AQ sensors and for all the three reference air quality stations. This result highlights the importance of policies aiming at reducing NO_2 emissions, as those implemented in the BrennerLEC project.

It is well known that pollutant concentrations in the atmosphere are controlled by the emission rates and by the interaction between dispersion and meteorological processes. In particular, NO_2 levels close to a highway follow typical daily and weekly cycles mostly related to the traffic flow. Figs. 8–10 show, for different sensors, the same types of graphics:

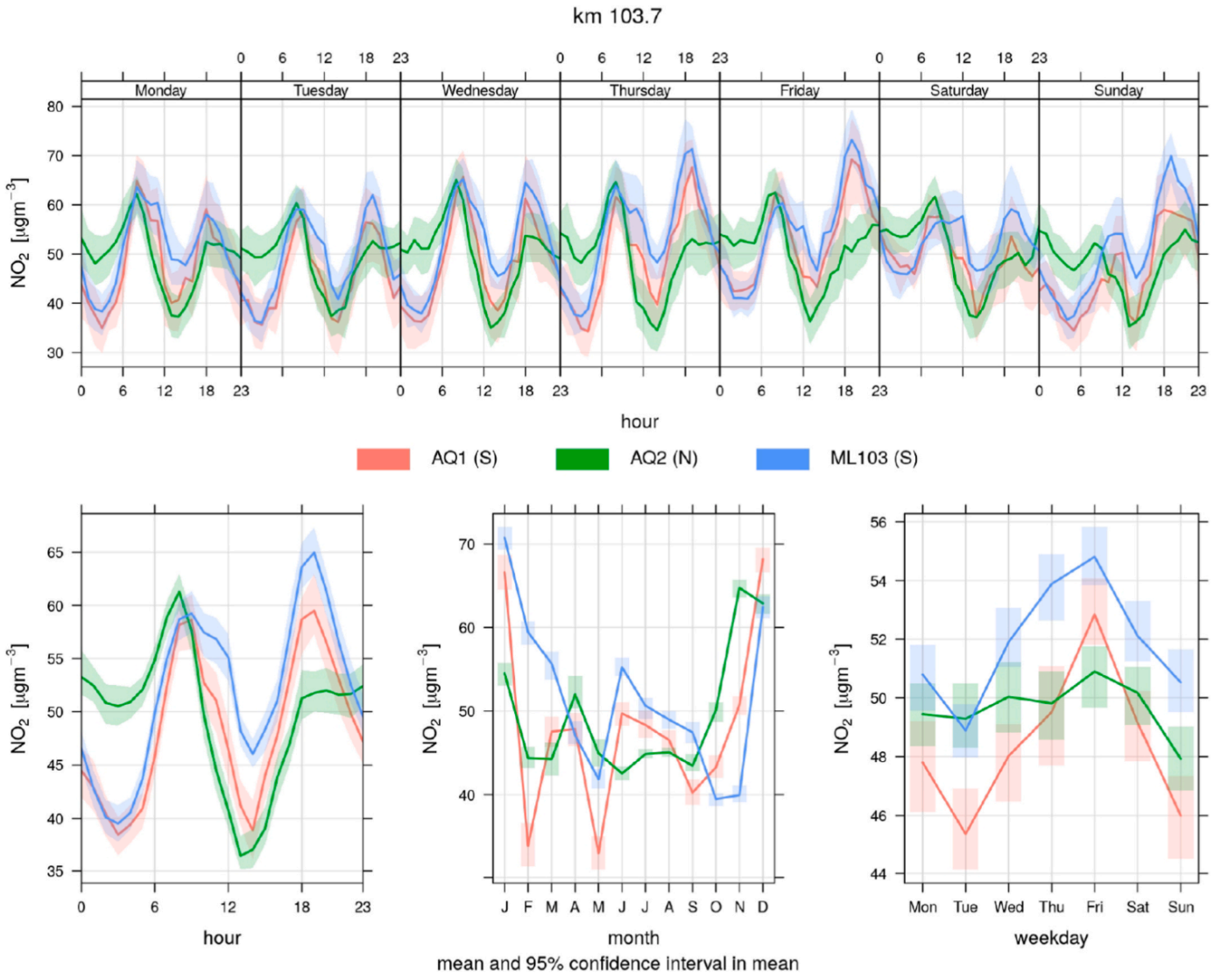

Fig. 8. NO_2 time variation plots of AQ1, AQ2 sensors and ML103 reference station throughout the one-year validation. The legend displays within round brackets the carriageway side where the measuring instruments are placed.

- the average diurnal cycles for each day of the week (top panel)
- the average diurnal cycle considering all the data (bottom left panel)
- the yearly cycle on a monthly basis (bottom center panel)
- the weekly cycle on a daily basis (bottom right panel)

In all the graphics the shaded areas represent the 95% confidence intervals.

Figs. 8 and 9 confirm that AQ1 and AQ3 are able to reproduce reasonably well the measurements of the reference stations ML103 and BL164, considering in particular the cyclic variability of NO_2 at different temporal scales. Daily and weekly NO_2 trends are consistent with the cyclic variations of traffic volumes along the A22 highway (see Fig. 11). The daily patterns show the two typical peaks of NO_2 concentration, one in the morning and one in the early evening. The peaks are driven by the diurnal cycle of traffic, which presents higher volumes at the beginning and at the end of the working day. The peaks in NO_2 concentrations are less pronounced on weekend days, when the heavy vehicles circulation is subject to restrictions (Fig. 11). The annual trend shows the characteristic higher NO_2 concentrations during wintertime. As highlighted in Section 2.5, this wintertime maximum is to be ascribed mainly to meteorological conditions, rather than to enhanced emissions, due to the presence of very stable stratifications with frequent ground-based temperature inversions. In fact, close to the highway the controlling source is the traffic, that does not show any wintertime peak (see Fig. 11), except during the Christmas holidays. On the other hand, during cold months, emissions from domestic heating are certainly higher, but they are expected to play a minor role on NO_2 concentrations close to the highway. Furthermore, during wintertime the conversion of traffic-emitted NO to NO_2 is facilitated by stagnant air conditions, while the weak solar radiation inhibits the splitting of NO_2 into NO and O (see e.g. Roberts-Semple et al., 2012). The top and bottom-left panels of Fig. 8 show that the evening peaks of the AQ2 sensor installed along the North carriageway are lower compared to measurements along the South carriageway (AQ1 and ML103). This is not observed in the morning peaks. Fig. 11 shows that this trend is not ascribable to the traffics volumes on the North and South carriageways, as they are similar. The difference is likely due to the fact that the stretch of the Brenner highway where these sensors are installed (i.e. at km 103.7) is SW-NE oriented (see Fig. 1). As mentioned in Section 2.5, up-valley winds (blowing from South) prevails during the day. Hence the sensors along the North carriageway are upwind with respect to the emission source, resulting in a local reduction of NO_2 concentration levels in contrast to the South carriageway. On the contrary, at night concentrations measured by AQ2 (North carriageway) are higher than those

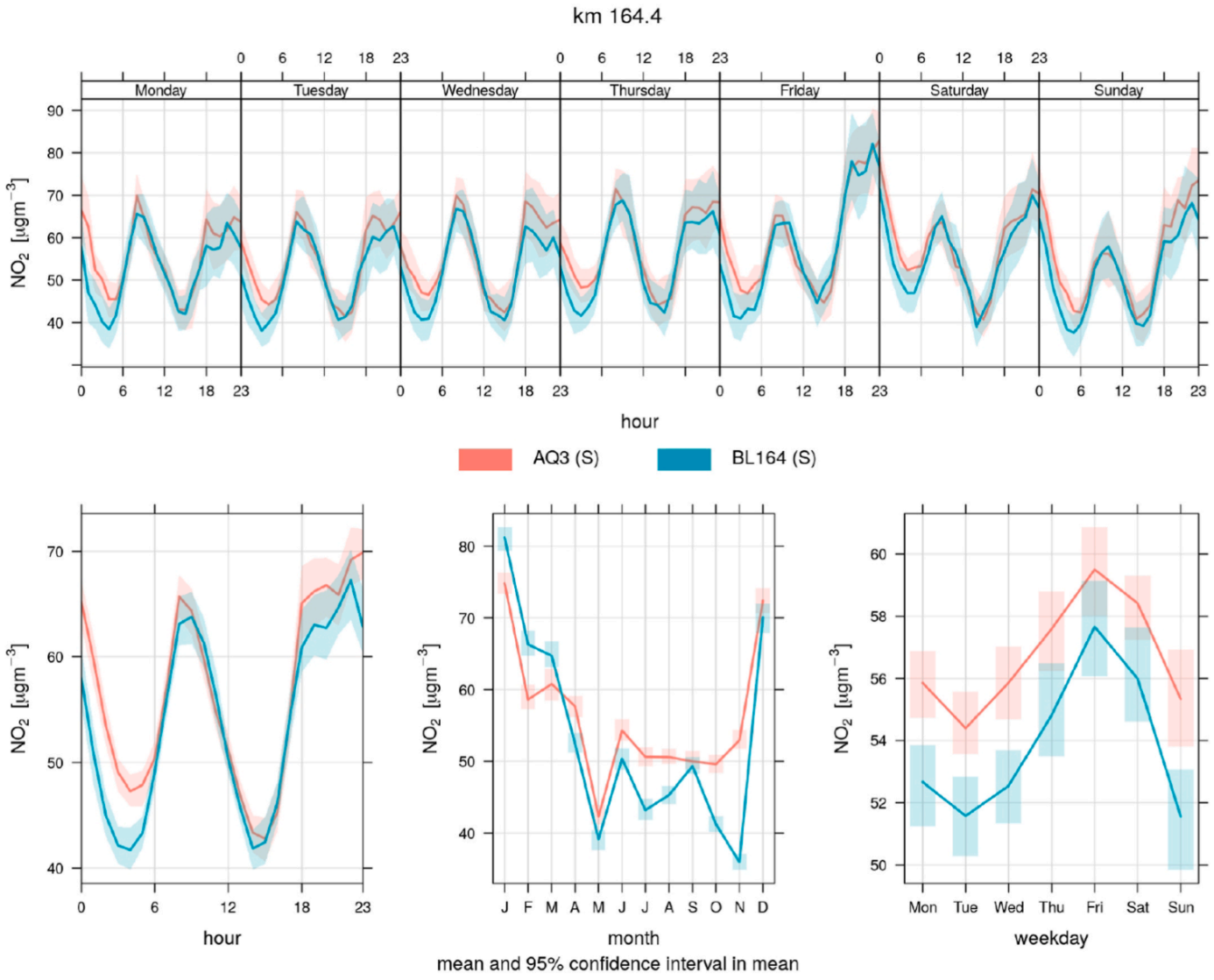

Fig. 9. NO_2 time variation plots of AQ3 sensor and BL164 reference station throughout the one-year validation. The legend displays within round brackets the carriageway side where the measuring instruments are placed.

measured by AQ1 and ML103 (South carriageway), as downvalley winds (from North) typically blows during nighttime.

Fig. 10 allows to examine the variation of NO_2 concentration with height. The two sensors AQ5 and AQ8 (10 m and 4 m above the ground level respectively) measure very similar values. Several effects has to be considered to explain the behavior of NO_2 levels so close to the source along the highway. The key components are likely the interaction of vehicle-induced turbulence with the mean flow near the highway and the buoyant rise of the exhaust gas mixture. In particular, the vehicle-induced turbulence may favour the development of a well-mixed layer close to the ground, thus explaining similar concentrations at different heights. However, further investigations are ongoing to ascertain a correct understanding.

Finally, given the availability of meteorological data from the reference stations, polar plots have been generated using the "polarPlot" Openair function (Carslaw, 2019), in order to analyze the relation between wind speed and direction and NO_2 concentrations. In the polar plot the wind speed is proportional to the radial distance, the wind direction is plotted according to the polar angle and the color scale represents the NO_2 hourly-averaged concentration.

Figs. 12 and 13 show respectively the polar plots for AQ1 and AQ3 (right panels), compared to ML103 and BL164 reference measurements (left panels) for the whole year of validation. AQ1 and AQ3 capture reasonably well the behavior of NO_2 concentrations of the reference stations, albeit both low-cost sensors tend to overestimate the lowest values and to underestimate the highest ones, especially considering AQ3. The polar plots indicate that the highest NO_2 levels occur under low wind speed conditions, as expected. Moreover, they clearly show that NO_2 concentrations are higher when sensors are downwind with respect to the highway, which runs from SW to NE both at km 103.3 and at km 164.4. The role of valley winds is even more recognizable when comparing NO_2 concentration patterns collected along the South and the North carriageways, i.e. considering the comparisons between ML103 and AQ2 in Fig. 12 and between ML107 and AQ4 in Fig. 14. They indeed exhibit symmetrical patterns with respect to the highway orientation, which are consistent with the variation of the along-valley wind direction and hence of the leeward side of the highway. Also, the AQ sensors along the North carriageway measure lower values of concentration, as they are downwind with respect to the emission source during nighttime, when the traffic load decreases substantially. Therefore the polar plots confirm the strict relation between NO_2 levels and valley winds, as also evidenced by the time variation plots.

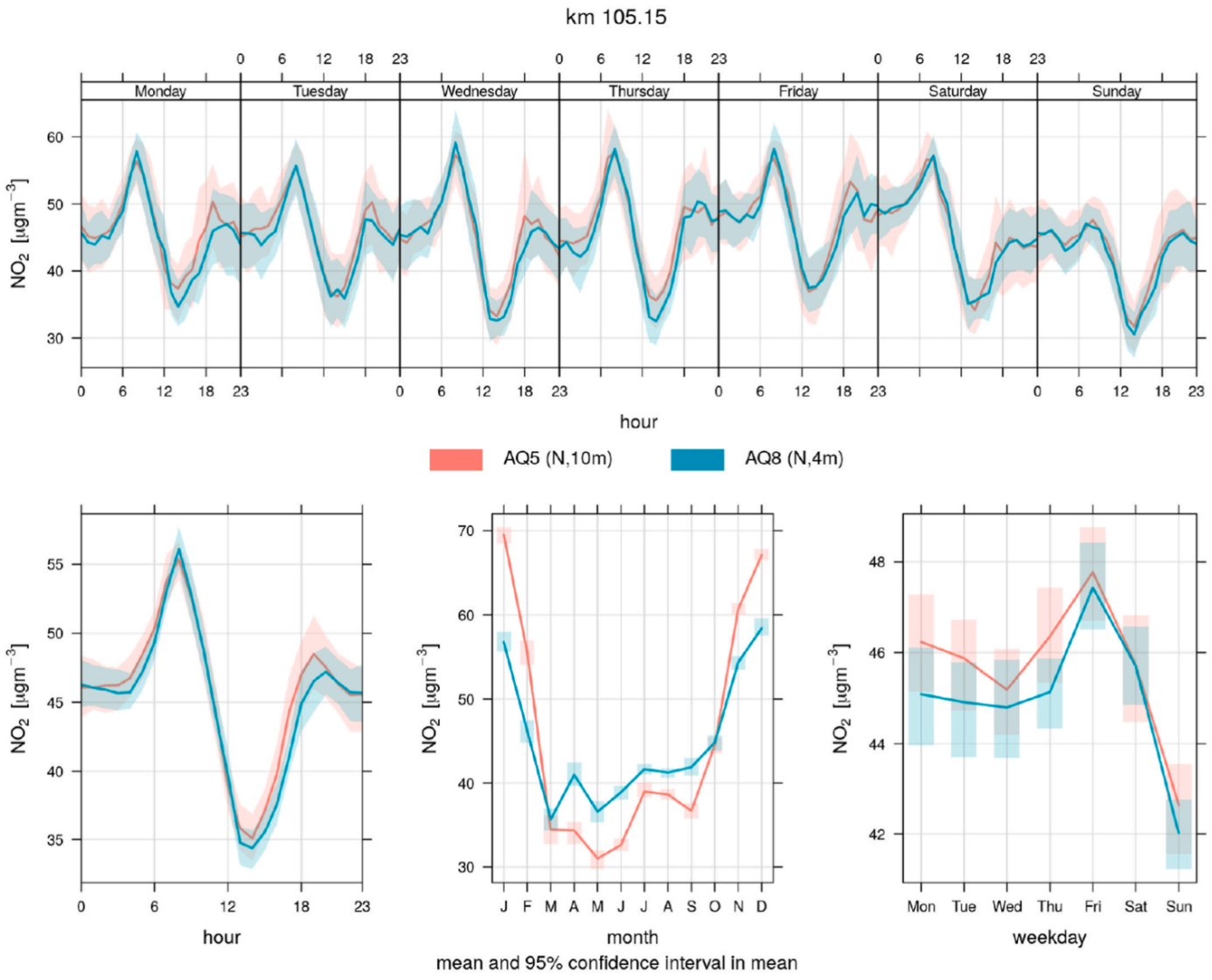

Fig. 10. NO_2 time variation plots of AQ5 and AQ8 sensors throughout the one-year validation. The legend displays within round brackets the carriageway side and the height where the measuring instruments are placed.

6. Conclusions

This work aimed at assessing the performance of a network of 10 low-cost electrochemical sensors in monitoring NO_2 concentration levels alongside the Brenner highway, one the most important Alpine corridor for freight transportation. The low-cost electrochemical sensors are part of the AirQino system, a custom-made printed circuit board, which integrates a set of commercial low-cost sensors for various meteorological, aerosol and gaseous measurements. It was shown that the choice of the regression model and of the parameters adopted plays a key role for suitably calibrating the low-cost sensors, as the raw measures are substantially affected by different environmental factors, which have to be properly taken into account. We tested four calibration models: two multivariate regressions (one standard and one with temperature-conditioned coefficients), a spline interpolation and a random forest algorithm. As may be expected, the more advanced models, i.e. the latter two, showed the best agreement. However, results obtained from the calibration phase highlighted that the performance of a simple multivariate regression was comparable to the more sophisticated models in terms of performance metrics, when the regression coefficients are adapted to vary with the temperature. In particular, two different sets of calibration parameters were obtained, depending on the internal temperature measured by the low-cost sensors. Hence, after testing the four models, we adopted this type of regression as the best compromise between complexity and performance. It is worth highlighting that all the calibration algorithms tested in the present work depend only on measurements performed by the AirQino system itself, in order to make the procedure independent from external measurements and thus easily exportable also to other contexts. The performance of the low-cost sensors was then evaluated during a year-long field campaign, by means of comparison against reference air quality stations. As expected, the statistical performance metrics slightly deteriorated with respect to the calibration periods, but the overall accuracy remained satisfactory. In particular, the low-cost sensors showed a low level of drift during the yearly measurement campaign, which is a remarkably long period for this kind of sensors. The analysis showed that the low-cost sensors were able to reproduce the typical temporal variability of NO_2 concentrations, considering daily, weekly and yearly cycles. These trends were consistent with the traffic volumes registered by inductive-loop detectors along the highway. Moreover, the low-cost sensors were capable of capturing the different patterns of the NO_2 concentration field along North and South carriageways. In particular, concentrations displayed a symmetrical dependence on wind direction on the two sides of the highway, highlighting that daily-periodic

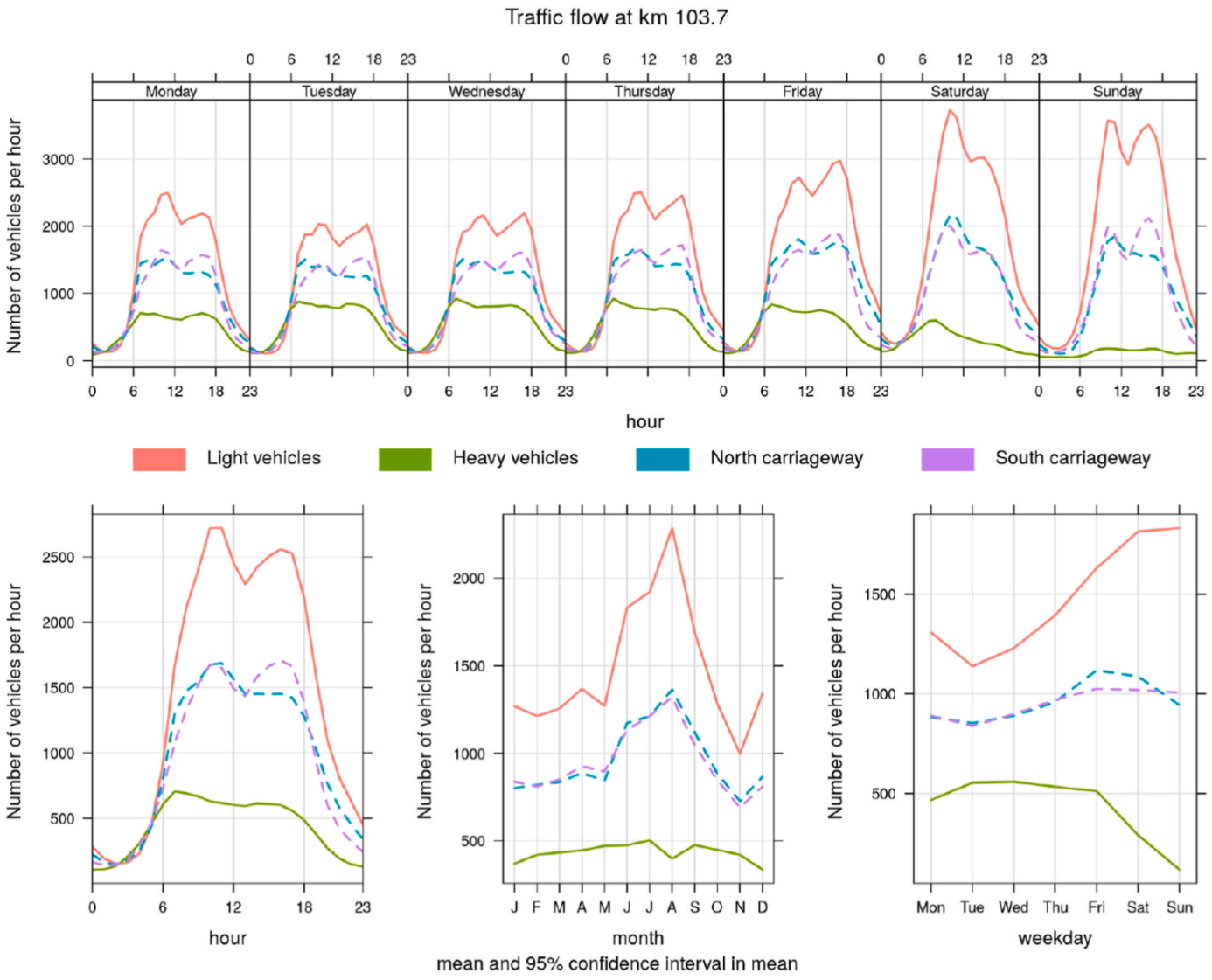

Fig. 11. Average hourly traffic volumes throughout the year of validation registered by an inductive-loop detector at km 103.7 of the Brenner highway and split by light/heavy vehicles (solid lines) and North/South carriageways (dashed lines).

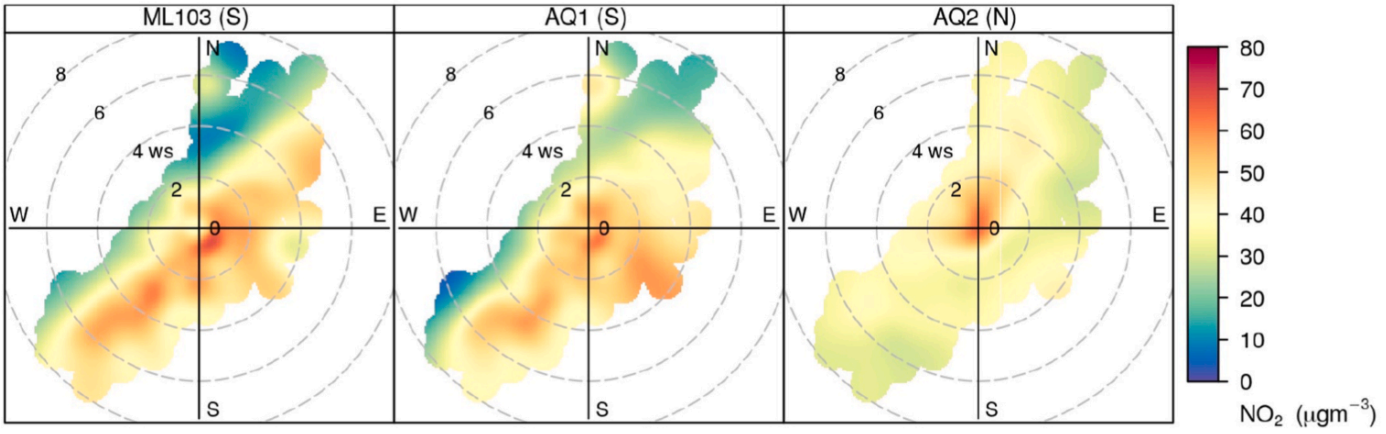

Fig. 12. NO_2 polar plots of ML103, AQ1 and AQ2 NO_2 concentrations throughout the year-long validation.

thermally-driven circulations play a crucial role in modulating pollutant concentrations close to major roads located in valleys. The results of this study pointed out that low-cost sensors can be a valuable solution to complement reference air quality measurements, providing the possibility to reach a wider spatial coverage and to monitor pollutant concentrations in critical situations, where standard measurements are

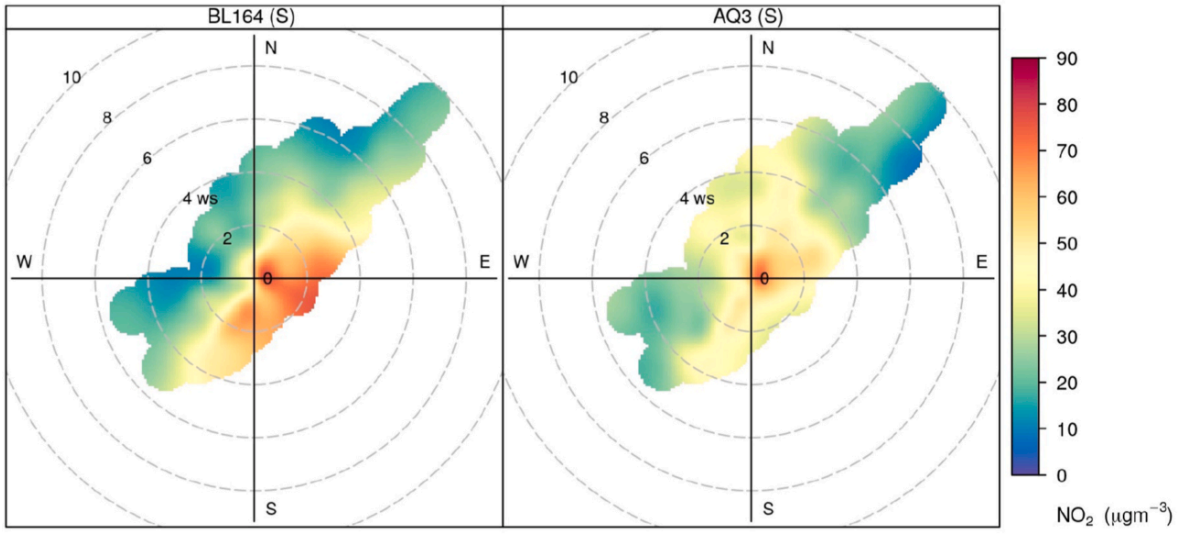

Fig. 13. NO_2 polar plots of BL164 and AQ3 NO_2 concentrations throughout the year-long validation.

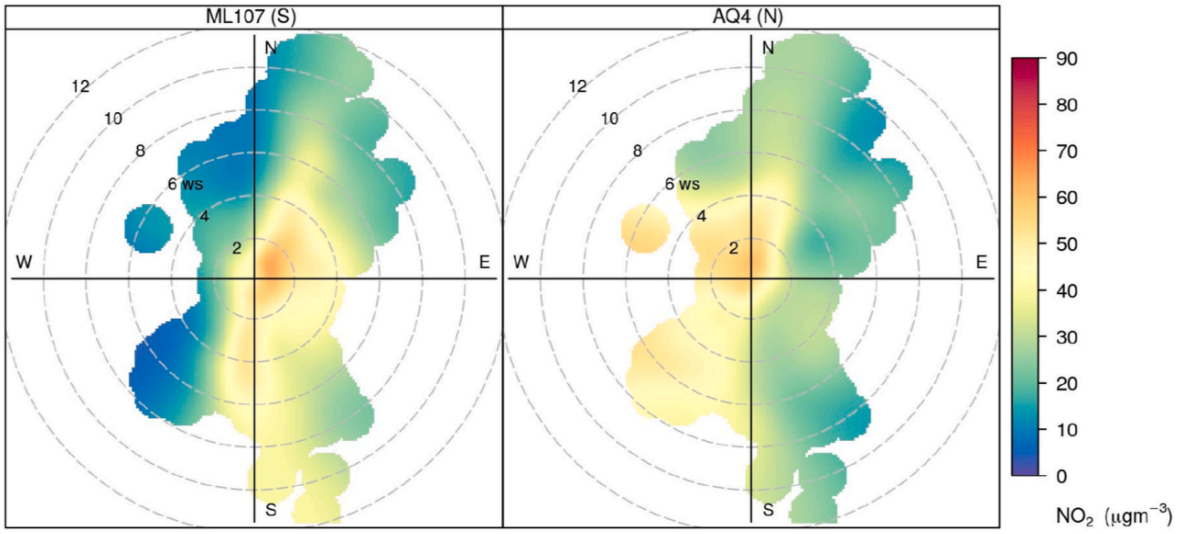

Fig. 14. NO_2 polar plots of ML107 and AQ4 NO_2 concentrations throughout the year-long validation.

usually not feasible. However, it is also highlighted that an expert management of this kind of sensors is needed, in order to continuously evaluate the goodness of the calibration and to detect possible failures. In particular, an automatic data quality procedure should be implemented in order to early detect possible drifts. To this regard, this study demonstrated the long-term stability of the sensors tested, under remarkably different environmental conditions. However, further investigations are needed to investigate more in detail this aspect, which is crucial for a widespread diffusion of this kind of sensors.

CRediT authorship contribution statement

Andrea Bisignano: Conceptualization, Methodology, Formal analysis, Writing – original draft, preparation. **Federico Carotenuto:** Resources, Writing – review & editing. **Alessandro Zaldei:** Resources, Writing – review & editing. **Lorenzo Giovannini:** Data curation, Conceptualization, Methodology, Supervision, Writing – review & editing.

Declaration of competing interest

The authors declare that they have no known competing financial interests or personal relationships that could have appeared to influence the work reported in this paper.

Acknowledgments

The authors would like to thank all partners of BrennerLec project for their technical support and useful suggestions. In particular special thanks go to Roberto Cavaliere (NOI Techpark), Ilaria De Biasi (Autostrada del Brennero S. p.A.), Valentina Miotto and Selene Cattani (APPA-TN), Gianluca Antonacci and Ilaria Todeschini (CISMA srl), Massimo Guariento and Patrick Dalpiaz (APPA-BZ). The authors would like to acknowledge APPA-TN and APPA-BZ for providing air quality and meteorological data from their weather stations.

Appendix A. Supplementary data

Supplementary data to this article can be found online at https://doi.org/10.1016/j.atmosenv.2022.119008.

References

Alphasense, 2019. No2-a43f Nitrogen Dioxide Sensor 4-Electrode Technical Specification. Alphasense Ltd.. Technical Report. http://www.alphasense.com/WEB1213/wp-content/uploads/2019/09/NO2-A43F.pd

Boehmke, B., Greenwell, B., 2019. Hands-On Machine Learning with R. https://doi.org/10.1201/9780367816377.

Borrego, C., Costa, A., Ginja, J., Amorim, M., Coutinho, M., Karatzas, K., Sioumis, T., Katsifarakis, N., Konstantinidis, K., De Vito, S., Esposito, E., Smith, P., Andre, N., Gerard, P., Francis, L., Castell, N., Schneider, P., Viana, M., Minguillon, M., Reimringer, W., Otjes, R., von Sicard, O., Pohle, R., Elen, B., Suriano, D., Pfister, V., Prato, M., Dipinto, S., Penza, M., 2016. Assessment of air quality microsensors versus reference methods: the eunetair joint exercise. Atmos. Environ. 147, 246–263. https://doi.org/10.1016/j.atmosenv.2016.09.050.

Botchkarev, A., 2019. A new typology design of performance metrics to measure errors in machine learning regression algorithms. Interdiscipl. J. Inf. Knowl. Manag. 14 https://doi.org/10.28945/4184, 45-7.

Breiman, L., 2001. Random forests. Mach. Learn. 45, 5–32.

Carotenuto, F., Brilli, L., Gioli, B., Gualtieri, G., Vagnoli, C., Mazzola, M., Viola, A., Vitale, V., Severi, M., Traversi, R., Zaldei, A., 2020. Long-term performance assessment of low-cost atmospheric sensors in the arctic environment. Sensors 20, 1919. https://doi.org/10.3390/s20071919.

Carslaw, D.C., 2019. The Openair Manual Open-Source Tools for Analysing Air Pollution Data. Manual for Version 2.6-6. University of York. https://davidcarslaw.com/files/openairmanual.pdf.

Carslaw, D.C., Ropkins, K., 2012. Openair - an r package for air quality data analysis. Environ. Model. Software 27–28.

Cavaliere, A., Carotenuto, F., Gennaro, D., Gioli, F., Gualtieri, B., Martelli, G., 2018. Development of low-cost air quality stations for next generation monitoring networks: calibration and validation of pm2.5 and pm10 sensors. Sensors 18. https://doi.org/10.3390/s18092843.

Cavallaro, F., Sommacal, G., 2018. Analysis Report of Projects, Policies, Strategies and Support Measures in the Field of CT Relevant for the Alpine Space. Deliverable D. T..1. Technical Report. Alpine Innovation for Combined Transport. https://www.alpine-space.eu/projects/alpinnoct/outputs/alpinnoct dt1.1.1.pdf.

Chambers, J.M., Hastie, T.J., Pregibon, D., 1990. Statistical Models in S. Physica Verlag HD, Heidelberg.

Chang, J.C., Hanna, S.R., 2004. Air quality model performance evaluation. Meteorol. Atmos. Phys. 87, 167–196.

Chang, J.C., Hanna, S.R., 2005. Technical descriptions and user's guide for boot statistical model evaluation software package. www.harmo.org/kit.

Clements, A.L., Griswold, W.G., Johnston, J.E., Herting, M.M., Thorson, J., Collier-Oxandale, A., Hannigan, M., 2017. Low-cost air quality monitoring tools: from research to practice (a workshop summary). Sensors 17. https://doi.org/10.3390/s17112478. https://www.mdpi.com/1424-8220/17/11/2478.

Concas, F., Mineraud, J., Lagerspetz, E., Varjonen, S., Liu, X., Puolamaki, K., Nurmi, P., Tarkoma, S., 2021. Low-cost Outdoor Air Quality Monitoring and Sensor Calibration: a Survey and Critical Analysis arXiv:1912.6384.

Cordero, J.M., Borge, R., Adolfo, N., 2018. Using statistical methods to carry out in field calibrations of low cost air quality sensors. Sensor. Actuator. B Chem. 267, 245–254.

De Vito, S., Piga, M., Martinotto, L., Francia, D., 2009. Co, no2 and nox urban pollution monitoring with on-field calibrated electronic nose by automatic bayesian regularization. Sensor. Actuator. B Chem. 143, 182–191. https://doi.org/10.1016/j.snb.2009.08.041.

e2v, 2008. MiCS-2710 Datasheet. Technical Report. e2v technologies. https://datasheetspdf.com/pdf-file/1041778/e2v/MiCS-2710/1.

EEA, a. Do lower speed limits on motorways reduce fuel consumption and pollutant emissions? URL: https://www.eea.europa.eu/themes/transport/speed-limits-fuel-consumption-and/speed-limits.

EEA, b. Emissions of air pollutants from transport. URL: https://www.eea.europa.eu/data-and-maps/indicators/transport-emissions-of-air-pollutants-8/..

EPA-AU, 2008. Site Contamination: Determination of Background Concentrations. Environment Protection Authority, South Australia. Technical Report. https://www.epa.sa.gov.au/files/13545_sc_background_concentrations.pdf.

EPA-US, 2020. List of Designated Reference and Equivalent Methods. United States Environmental Protection Agency. Technical Report. https://www.epa.gov/sites/production/files/2019-08/documents/designated_reference_and-equivalent_methods.pdf.

Esposito, E., De Vito, S., Salvato, M., Bright, V., Jones, R.L., Popoola, O., 2016. Dynamic neural network architectures for on field stochastic calibration of indicative low cost air quality sensing systems. Sensor. Actuator. B Chem. 231, 701–713. https://doi.org/10.1016/j.snb.2016.03.038.

Falocchi, M., Tirler, W., Giovannini, L., Tomasi, E., Antonacci, G., Zardi, D., 2020. A dataset of tracer concentrations and meteorological observations from the bolzano tracer experiment (btex) to characterize pollutant dispersion processes in an alpine valley. Earth Syst. Sci. Data 12, 277–291. https://doi.org/10.5194/essd-12-277-2020.

Fritsch, F.N., Carlson, R.E., 1980. Monotone piecewise cubic interpolation. SIAM J. Numer. Anal. 17, 238–246. https://doi.org/10.1137/0717021.

Giovannini, L., Ferrero, E., Karl, T., Rotach, M.W., Staquet, C., Castelli, T., Zardi, S., Atmospheric, D., 2020. Atmospheric pollutant dispersion over complex terrain: challenges and needs for improving air quality measurements and modeling. Atmosphere 11. https://doi.org/10.3390/atmos11060646. https://www.mdpi.com/2073-4433/11/6/646.

Giovannini, L., Laiti, L., Serafin, S., Zardi, D., 2017. The thermally driven diurnal wind system of the adige valley in the Italian alps. Q. J. R. Meteorol. Soc. 143, 2389–2402. https://doi.org/10.1002/qj.3092.

Gualtieri, G., Camilli, F., Cavaliere, A., De Filippis, T., Gennaro, D., Lonardo, F.D., Dini, S., Gioli, F., Matese, B., Nunziati, A., Rocchi, W., Vagnoli, P., Zaldei, C., 2017. An integrated low-cost road traffic and air pollution monitoring platform to assess vehicles' air quality impact in urban areas. Transport. Res. Proc. 27, 609–616. https://doi.org/10.1016/j.trpro.2017.12.043, 20th EURO Working Group on Transportation Meeting, EWGT 2017, 4-6 September 2017, Budapest, Hungary.

Heimann, I., Bright, V.B., McLeod, M.W., Mead, M.I., Popoola, O.A.M., Stewart, G.B., Jones, R.L., 2015. Source attribution of air pollution by spatial scale separation using high spatial density networks of low cost air quality sensors. Atmos. Environ. 113, 10–19. https://doi.org/10.1016/j.atmosenv.2015.04.057.

Horiba, APNA-370 Ambient NOx Monitor. Technical Report. Horiba, Ltd. URL: https://www.horiba.com/en_en/products/detail/action/show/Product/apna-370-451/.

Karagulian, F., Barbiere, M., Kotsev, A., Spinelle, L., Gerboles, M., Lagler, F., Redon, N., Crunaire, S., Borowiak, A., 2019. Review of the performance of low-cost sensors for air quality monitoring. Atmosphere 10. https://doi.org/10.3390/atmos10090506. https://www.mdpi.com/2073-4433/10/9/506.

LeGates, D.R., McCabe, G.J.A., 2013. Refined index of model performance: a rejoinder. Int. J. Climatol. 33, 1053–1056. https://doi.org/10.1002/joc.3487.

Liaw, A., Wiener, M., 2014. Package randomforest: Breiman and cutler's random forests for classification and regression. R Development Core Team 4, 6–10.

Masson, N., Piedrahita, R., Hannigan, M., 2015. Quantification method for electrolytic sensors in long-term monitoring of ambient air quality. Sensors 15, 27283–27302. https://doi.org/10.3390/s151027283.

Mijling, B., Jiang, Q., de Jonge, D., Bocconi, S., 2018. Field calibration of electrochemical NO_2 sensors in a citizen a science context. Atmos. Meas. Tech. 11, 1297–1312. https://doi.org/10.5194/amt-11-1297-2018. https://amt.copernicus.org/articles/11/1297/2018/.

Patryl, L., Galeriu, D., 2011. Statistical Performances Measures - Models Comparison. International Atomic Energy Agency. Technical Report.

Pederzoli, A., Thunis, P., Georgieva, E., Borge, R., Carruthers, D., Pernigotti, D., 2012. Performance criteria for the benchmarking of air quality model regulatory applications: the target approach. Int. J. Environ. Pollut. 50, 175–189.

Perperoglou, A., Sauerbrei, W., Abrahamowicz, M., Schmid, M., 2019. A review of spline function procedures in r. BMC Med. Res. Methodol. 9, 19–46.

Piedrahita, R., Xiang, Y., Masson, N., Ortega, J., Collier, A., Jiang, Y., Li, K., Dick, R.P., Lv, Q., Hannigan, M., Shang, L., 2014. The next generation of low-cost personal air quality sensors for quantitative exposure monitoring. Atmos. Meas. Tech. 7, 3325–3336. https://doi.org/10.5194/amt-7-3325-2014.

Popoola, O., Carruthers, D., Lad, C., Bright, V., Mead, M., Stettler, M., Saffell, J., Jones, R., 2018. Use of networks of low cost air quality sensors to quantify air quality in urban settings. Atmos. Environ. 194, 58–70. https://doi.org/10.1016/j.atmosenv.2018.09.030.

Popoola, O., Stewart, G., Mead, M., Jones, R., 2016. Development of a baseline-temperature correction methodology for electrochemical sensors and its implications for long-term stability. Atmos. Environ. 147, 330–343. https://doi.org/10.1016/j.atmosenv.2016.10.024.

R-Team, 2006. A Language and Environment for Statistical Computing. https://doi.org/10.1890/0012-9658(2002)083[3097:CFHIWS]2.0.CO;2.

Roberts-Semple, D., Song, F., Y, G., 2012. Y. seasonal characteristics of ambient nitrogen oxides and ground-level ozone in metropolitan northeastern New Jersey. Atmos. Pollut. Res. 3, 247–257.

Spinelle, L., Aleixandre, M., Gerboles, M., 2013. Protocol of Evaluation and Calibration of Low-Cost Gas Sensors for the Monitoring of Air Pollution. Joint Research Centre, Institute for Environment and Sustainability. https://doi.org/10.2788/9916. Technical Report.

Spinelle, L., Gerboles, M., Villani, M.G., Aleixandre, M., Bonavitacola, F., 2015. Field calibration of a cluster of low-cost available sensors for air quality monitoring. part a: ozone and nitrogen dioxide. Sensor. Actuator. B Chem. 215, 249–257. https://doi.org/10.1016/j.snb.2015.03.031.

Spinelle, L., Gerboles, M., Villani, M.G., Aleixandre, M., Bonavitacola, F., 2017. Field calibration of a cluster of low-cost commercially available sensors for air quality monitoring. part b: No, co and co2. Sensor. Actuator. B Chem. 238, 706–715. https://doi.org/10.1016/j.snb.2016.07.036.

Spuler, M., Sarasola-Sanz, A., Birbaumer, N., Rosenstiel, W., Ramos-Murguialday, A., 2015. Comparing metrics to evaluate performance of regression methods for decoding of neural signals. In: Conference Proceedings: Annual International Conference of the IEEE Engineering in Medicine and Biology Society. IEEE Engineering in Medicine and Biology Society. Conference, pp. 1083–1086. https://doi.org/10.1109/EMBC.2015.7318553.

Taylor, K.E., 2001. Summarizing multiple aspects of model performance in a single diagram. J. Geophys. Res. 106, 7183–7192.

Thunis, P., Pederzoli, A., Pernigotti, D., 2012. Performance criteria to evaluate air quality modeling applications. Atmos. Environ. 59, 476–482.

Tomasi, E., Giovannini, L., Falocchi, M., Antonacci, G., Jimenez, P.A., Kosovic, B., Alessandrini, S., Zardi, D., Monache, D., Ferrero, L., Turbulence, E., 2019. Turbulence parameterizations for dispersion in sub-kilometer horizontally non-homogeneous flows. Atmos. Res. 228, 122–136. https://doi.org/10.1016/j.atmosres.2019.05.018.

Tomasi, E., Giovannini, L., Zardi, D., de Franceschi, M., 2017. Optimization of noah and noah-mp wrf land surface schemes in snow – melting conditions over complex terrain. Mon. Weather Rev. 145 https://doi.org/10.1175/MWRD160408.1.

Unitec, 2018. SENS-IT Technical Datasheet. Unitec s.r.l. Technical Report. http://www.unitec-srl.com/site/products/sens-it/.

Watson, J., Thurston, G., Frank, N., Lodge, J., Wiener, R., McElroy, F., Kleinman, M., Mueller, P.K., Schmidt, A., Lipfert, F., Thompson, R., Dasgupta, P., Marrack, D., Michaels, R., Moore, T., Penkala, S., Tombach, I., Vestman, L., Hauser, T., Chow, J., 1995. Measurement methods to determine compliance with ambient air quality standards for suspended particles. J. Air Waste Manag. Assoc. 45, 666–684. https://doi.org/10.1080/10473289.1995.10467395.

Wilks, D.S., 2019. Chapter 7 - statistical forecasting. In: Statistical Methods in the Atmospheric Sciences, fourth ed. Elsevier, pp. 235–312. https://doi.org/10.1016/B978-0-12-815823-4.00007-9. fourth edition.

Willmott, C.J., Robeson, S.M., Matsuuraa, K.A., 2012. A refined index of model performance. Int. J. Climatol. 32, 2088–2094. https://doi.org/10.1002/joc.2419.

WMO, 2018. Guide to Instruments and Methods of Observation - Volume I - Measurement of Meteorological Variables. URL:. Word Meteorological Organization. Technical Report. https://library.wmo.int/doc_num.php?explnum_id=10179.

Zaldei, A., Camilli, F., De Filippis, T., Gennaro, D., Lonardo, F.D., Dini, S., Gioli, F., Gualtieri, B., Matese, G., Nunziati, A., 2017. An integrated low-cost road traffic and air pollution monitoring platform for next citizen observatories. Transport. Res. Proc. 24, 531–538. https://doi.org/10.1016/j.trpro.2017.06.002, 3rd Conference on Sustainable Urban Mobility, 3rd CSUM 2016, 26 - 27 May 2016, Volos, Greece.

Zikova, N., Hopke, P.K., Ferro, A.R., 2017a. Evaluation of new low-cost particle monitors for pm2.5 concentrations measurements. J. Aerosol Sci. 105, 24–34. https://doi.org/10.1016/j.jaerosci.2016.11.010.

Zikova, N., Masiol, M., Chalupa, D.C., Rich, D.Q., Ferro, A.R., Hopke, P.K., 2017b. Estimating hourly concentrations of pm2.5 across a metropolitan area using low-cost particle monitors. Sensors 17. https://doi.org/10.3390/s17081922.

Zimmerman, N., Presto, A.A., Kumar, S.P.N., Gu, J., Hauryliuk, A., Robinson, E.S., Robinson, A.L., Subramanian, R.A., 2018. A machine learning calibration model using random forests to improve sensor performance for lower-cost air quality monitoring. Atmos. Meas. Tech. 11, 291–313. https://doi.org/10.5194/amt-11-291-2018.

Andrea Bisignano is a Research Fellow at the University of Trento, teaching Air Pollution Modelling. He works in pollutant dispersion using Lagrangian stochastic models. He is a master graduate in Physics of Complex Systems from University of Turin, with a PhD from University of Eastern Piedmont in Environmental Sciences.

Federico Carotenuto obtained a PhD in Biology from the University of Innsbruck and is now a research fellow at the Institute for BioEconomy of CNR. His main research interests are surface to atmosphere exchanges of biological particles and non-biological atmospheric pollutants.

Alessandro Zaldei, responsible for "Urban Climate Laboratory". His main research interests are urban climate, surface to atmosphere gas exchanges and air quality monitoring. Expertise in environmental monitoring and sensors development.

Lorenzo Giovannini is assistant professor at the Department of Civil, Environmental and Mechanical Engineering of the University of Trento (Italy). His research activity focuses mainly on the analysis of atmospheric processes typical of mountainous regions and on the evaluation of microclimatic alterations induced by urban areas, by means of both experimental campaigns and numerical meteorological models. He is involved in different research projects, covering several aspects of applied meteorology, such as pollutant dispersion, support to agricultural practices, estimation of renewable energy sources and optimization of building energy consumption.